



Lead sorption by biochar produced from digestates: Consequences of chemical modification and washing

Suchanya Wongrod, Stéphane Simon, Gilles Guibaud, Piet N.L. Lens, Yoan Pechaud, David Huguenot, Eric D. van Hullebusch

► To cite this version:

Suchanya Wongrod, Stéphane Simon, Gilles Guibaud, Piet N.L. Lens, Yoan Pechaud, et al.. Lead sorption by biochar produced from digestates: Consequences of chemical modification and washing. Journal of Environmental Management, 2018, 219, pp.277-284. 10.1016/j.jenvman.2018.04.108 . hal-02141756

HAL Id: hal-02141756

<https://hal.science/hal-02141756>

Submitted on 28 May 2019

HAL is a multi-disciplinary open access archive for the deposit and dissemination of scientific research documents, whether they are published or not. The documents may come from teaching and research institutions in France or abroad, or from public or private research centers.

L'archive ouverte pluridisciplinaire **HAL**, est destinée au dépôt et à la diffusion de documents scientifiques de niveau recherche, publiés ou non, émanant des établissements d'enseignement et de recherche français ou étrangers, des laboratoires publics ou privés.

Lead sorption by biochar produced from digestates: Consequences of chemical modification and washing

Suchanya Wongrod^{a,b,c}, Stéphane Simon^c, Gilles Guibaud^{c,*}, Piet N.L. Lens^b, Yoan Pechaud^a, David Huguenot^a, Eric D. van Hullebusch^{a,b}

^a Université Paris-Est, Laboratoire Géomatériaux et Environnement (EA 4508), UPEM, 77454, Marne-la-Vallée, France

^b IHE Delft Institute for Water Education, P.O. Box 3015, 2601 DA Delft, The Netherlands

^c Université de Limoges, PEIRENE-Groupement de Recherche Eau Sol Environnement (EA 7500), Faculté des Sciences et Techniques, 123 avenue Albert Thomas, 87060 Limoges, France

*Corresponding author: gilles.guibaud@unilim.fr

Abstract

The main objectives of this work are to investigate the consequences of different chemical treatments (*i.e.* potassium hydroxide (KOH) and hydrogen peroxide (H₂O₂)) and the effect of biochar washing on the Pb sorption capacity. Biochars derived from sewage sludge digestate and the organic fraction of municipal solid waste digestate were separately modified with 2 M KOH or 10% H₂O₂ followed by semi-continuous or continuous washing with ultrapure water using batch or a column reactor, respectively. The results showed that the Pb adsorption capacity could be enhanced by chemical treatment of sludge-based biochar. Indeed, for municipal solid waste biochar, the Pb maximum sorption capacity was improved from 73 mg g⁻¹ for unmodified biochar to 90 mg g⁻¹ and 106 mg g⁻¹ after H₂O₂ and KOH

treatment, respectively. In the case of sewage sludge biochar, it increased from 6.5 mg g^{-1} (unmodified biochar) to 25 mg g^{-1} for H_2O_2 treatment. The sorption capacity was not determined after KOH treatment, since the Langmuir model did not fit the experimental data. The study also highlights that insufficient washing after KOH treatment can strongly hinder Pb sorption due to the release of organic matter from the modified biochar. This organic matter may interact in solution with Pb, resulting in an inhibition of its sorption onto the biochar surface. Continuous column-washing of modified biochars was able to correct this issue, highlighting the importance of implementing a proper treated biochar washing procedure.

Keywords biochar, digestate, sorption, organic sludge, lead

1. Introduction

Metal pollution is of very high concerns for human health due to their persistence and toxicity in the environment even in low concentrations. Lead (Pb) has been recognized as one of the most toxic metals in Europe (Tóth et al., 2016). Pb pollution often originates from smelters, mining, industrial discharges, car batteries and Pb-based piping for water supply. Discharge of untreated wastewater from the industry may cause an adverse effect to animals and humans. One study reported a case of severe Pb poisoning of children in Haina (Dominican Republic), attributed to a car battery recycling factory (Kaul et al., 1999). Many conventional treatment methods have been developed to decrease Pb levels in contaminated water, including chemical precipitation, coagulation, ion exchange and adsorption (Inyang et al., 2015).

Lead sorption by activated carbon (Cechinel et al., 2014), agricultural waste-derived biochars (*e.g.* pine wood or rice husk) (Liu & Zhang, 2009), natural zeolite and kaolinite clay (Andrejkovicova et al., 2016; Jiang et al., 2009) have been reported. Recent studies show the potential application of biochar in metal-polluted water treatment due to its high specific surface area and surface properties, *e.g.* surface charge and hydrophobicity (Liu & Zhang, 2009; Zielińska et al., 2015). Indeed, the solid organic by-product generated by anaerobic digestion of sludge from wastewater treatment plants has been considered as an alternative source of raw material to manufacture adsorbents (*i.e.* biochar) for metal removal (Zhang et al., 2013). Biochar is a black solid char derived from the pyrolysis of organic waste materials in a limiting oxygen environment (Inyang et al., 2015). Through the pyrolysis technology, it promotes the recycling of organic waste and supports the environmental sustainability for the community. Biochar has been widely used for many purposes in the environment, such as soil conditioner (Saifullah et al., 2018) or filtration medium in wastewater treatment (Mohan et al., 2014). However, there are only few studies on the use of organic by-product sludge

biochar to remove metals from water. Biochar produced from organic digested sludge has been used for As(V), Cd(II), Cr(III), Cu(II) and Ni(II) removal from water (Inyang et al., 2012; Jin et al., 2014). A few studies have been dedicated to the Pb sorption by sludge biochars, which can be found in the literature (Table S1).

The main mechanisms involved in Pb sorption onto the biochar are cation exchange, surface complexation, surface precipitation and physical adsorption (Ho et al., 2017; Li et al., 2017). Among these mechanisms, cation exchange of Pb with Ca^{2+} and Mg^{2+} is the main contributor to Pb sorption by sludge-based biochar, accounting for 40–52%. Exchanges can also occur to a lesser extend with K^+ and Na^+ (<8.5%) (Li et al., 2017), which is in a good agreement with the study of Lu et al. (2012). The surface complexation between Pb and surface functional groups of biochar (*e.g.* carboxyl and hydroxyl groups) also plays a major role, contributing for about 40% of Pb removal (Li et al., 2017). Surface precipitation can also occur since sludge biochars generally contain high amounts of phosphate (PO_4^{3-}) and carbonate (CO_3^{2-}) on their surface. Finally, the high surface area of biochar may favor physical adsorption of Pb onto biochar active pore sites (Agrafioti et al., 2014). The relative importance of these sorption mechanisms depends on the biochar feedstock.

Compared to activated carbon, the sorption capacity for Pb by biochar is low and thus numerous modification methods have been applied to improve it. The common treatment methods of biochar are physical activation with steam and chemical treatment with acids, oxidizing agents and alkali solutions (Sizmur et al., 2017). The steam activation of biochar is usually performed at high temperature (>800 °C), thus increasing the adsorbent cost which it is not feasible for large scale operation (Wang and Liu, 2018). The chemical modification of biochar is considered as an inexpensive technique since no heat is required during the operation. Treatment of biochar with KOH increases the surface hydroxyl groups and the basicity on the biochar surface (Fan et al., 2016; Li et al., 2014), dissolves ash and condenses

organic matter (*e.g.* lignin and celluloses) in the biochar (Lin et al., 2012; Liou & Wu, 2009; Liu et al., 2012). Modification of biochar with H₂O₂ was found to increase O-containing functional groups, particularly carboxyl groups, on the biochar surfaces (Rajapaksha et al., 2016). Such chemical modifications could induce a leaching of organic matter and mineral ash from biochar pore sites. Thus, after the treatment, several batch washing of the biochar with ultrapure water are required until the pH becomes stable or neutral (Huang et al., 2017; Regmi et al., 2012; Wu et al., 2017). Usually, batch washing of biochar is performed without any concerns on the release of organic or inorganic compounds (*e.g.* PO₄³⁻ and CO₃²⁻) from biochar. Since this can influence the sorption of metals by biochar, the effective elimination of these released compounds should be considered. Unfortunately, there is currently a lack of information on the effect of biochar washing on the elimination of the released compounds from biochar after chemical treatment.

This work aims to study the consequences of chemical treatments of biochar and subsequent washing conditions on the Pb sorption capacity. Two chemical reagents (*i.e.* KOH and H₂O₂) and two washing modes (semi-continuous batch washing as usually performed in the literature and continuous column washing) were applied to raw biochars from sewage sludge and the organic fraction of municipal solid waste. The consequences onto the Pb sorption were evaluated through adsorption kinetic and isotherm studies.

2. Materials and methods

2.1. Feedstocks and biochar preparation

Raw sewage sludge digestate (RSS) and raw organic fraction of municipal solid waste digestate (RMSW) were obtained separately from a wastewater treatment plant and from a solid waste treatment plant located in France. Biochar from RSS was industrially pyrolyzed at

350 °C for 15 min using the Biogreen® technology, while biochar from RMSW was produced at lab scale. Based on the study of Pituello et al. (2014), the RMSW was dried overnight at 65 °C to reduce the initial moisture content to less than 10%. After that, it was crushed and sieved into a particle size of 2 mm to separate impurities such as plastic bags, needles and glasses. The RMSW-derived biochar was produced at 400 °C using porcelain crucibles with lid-cover (Haldenwanger 79 MF, Germany) in a muffle furnace (heating rate 15 °C min⁻¹) for 1 h. The obtained materials were left to cool down at room temperature with the lids cover.

As recommended by Jin et al. (2014), Wu et al. (2017) and Xue et al. (2012), biochars were washed by semi-continuous means with ultrapure water for 3–4 times (*i.e.* 2 g of biochar per 200 mL of ultrapure water per washing) until a stable pH was obtained. The RSS-derived biochar produced at 350 °C and the RMSW-derived biochar produced at 400 °C are named as SS^{sem} and MSW^{sem}, respectively.

2.2. Biochar chemical modification

In this study, KOH and H₂O₂ were selected for the chemical modification of biochar due to the great enhancement of metal sorption (Rajapaksha et al., 2016). To prepare the modified biochar with H₂O₂, 2 g of biochar was placed into 20 mL of a 10% H₂O₂ solution and shaken at 25 (± 2) °C for 2 h (modified from Xue et al., 2012). Biochar treated with KOH was prepared by mixing 2 g biochar with 100 mL of 2 M KOH solution and was shaken at 25 (± 2) °C for 2 h (modified from Jin et al., 2014). The total mass of biochar used was around 10 g per each chemical treatment. After chemical modification, biochars were all semi-continuously washed with ultrapure water. Some biochars were submitted to a subsequent continuously washing to study the influence of the washing conditions.

For the semi-continuous washing, the chemically modified biochar was washed in batch by stirring 2 g of biochar in 200 mL of ultrapure water at 20 (\pm 2) °C. The batch washing was repeated for 3–4 times until the pH became stable (Jin et al., 2014; Wu et al., 2017; Xue et al., 2012). For the continuous washing, a part of the semi-continuous washed biochar was subsequently washed by continuous circulation of ultrapure water in a glass column (2.8 cm in diameter and 42.5 cm in height). A peristaltic pump (Ismatec Reglo Analog, Model No. ISM827, Ismatec SA Company, Switzerland) was used to maintain the up-flow velocity of 0.77 (\pm 0.01) cm min⁻¹. Glass beads (2 mm size) were used at the bottom of the column to generate the flow distribution. The column was flushed continuously for at least 70 h at 20 (\pm 2) °C with a hydraulic retention time of 6 h.

Once washed, the modified biochars were recovered using VWR filter papers, then dried in an oven at 50 °C overnight and further kept in a desiccator prior to use. The semi-continuously washed H₂O₂ and KOH-treated biochars are labeled as MSW-H₂O₂^{sem}, MSW-KOH^{sem}, SS-H₂O₂^{sem} and SS-KOH^{sem} for RMSW and SS based biochar, respectively. The continuously washed H₂O₂ and KOH-treated sewage sludge biochars are labeled as SS-H₂O₂^{con} and SS-KOH^{con}, respectively.

2.3. Biochar characterization

The pH of the biochar was measured using a pH meter (LPH 330T, Tacussel, France). A suspension of 1 g of sample in 20 mL of deionized water was stirred continuously for 5 min and let to suspend for 15 min.

To quantify the total content of metal(loid)s (*i.e.* Al, As, Cd, Cr, Cu, Ni, Pb, Mn, Fe and Zn) and cationic macroelements (*i.e.* Ca, K, Mg and Na) in biochar, an acid digestion was performed using H₂O₂ (30% w/w, Sigma-Aldrich) and concentrated HCl (37% w/w, Merck) and HNO₃ (65% w/w, Merck) according to EPA Method 3050B (EPA, 1996). The

digestion was carried out in a heating block at 95 (\pm 5) °C. After filtration with a Whatman grade 1 qualitative filter paper, trace elements were analyzed using inductively coupled plasma optical emission spectroscopy (ICP-OES) (Optima 8300, PerkinElmer, France).

An X-ray powder diffractometer (AXS D8, Bruker, Germany) was used to identify the crystalline structures of the biochars. Fourier transform infrared (FTIR) spectroscopy (IRAffinity-1, Shimadzu, Japan) was used to identify surface functional groups of biochar with a deuterated-triglycine sulfate (DTGS) detector. The details of the sample preparation for XRD and FTIR analysis are described in the Supplementary Information. Brunauer-Emmett-Teller (BET) specific surface area of chemically-modified biochar samples were determined using the N₂ adsorption method at 77 K (3Flex, Micromeritics, USA). Before BET analysis, the biochar samples were dried at 105 °C for 5 h.

2.4. Characterization of solution after column washing of biochar

During continuous washing of SS-KOH^{sem} and SS-H₂O₂^{sem}, liquid samples were collected at the outlet of the column over time to measure pH (LPH 330T, Tacussel, France), conductivity (CDM 210 conductivity-meter, Radiometer, Copenhagen, Denmark), dissolved organic carbon (DOC), PO₄³⁻, CO₃²⁻ and bicarbonate (HCO₃⁻). Dissolved organic carbon was determined using a TOC Analyzer (multi N/C® 2100S, Analytikjena, Germany) according to the standard method from Afnor (Afnor, 1997a). A colorimetric method (Afnor, 1997b) was used to measure PO₄³⁻ with a spectrophotometer (DR1900, Hach, France) at λ 700 nm. For CO₃²⁻ and HCO₃⁻, they were analyzed by a titrimetric method (Afnor, 1996) using 10⁻³ M HCl as a titrant and phenolphthalein and mixed bromocresol green-methyl red as indicators. Microwave Plasma Atomic Emission Spectroscopy (MP-AES) (Agilent 4100, Agilent Technologies Inc., USA) was used to analyze the released concentration of Ca and Mg at λ 422.673 nm and λ 285.213 nm, respectively.

2.5. Sorption experiments

A stock solution of 1000 mg L^{-1} Pb(II) was prepared from $\text{Pb}(\text{NO}_3)_2$. The solution was diluted in the range from 10 to 1000 mg L^{-1} and the initial solution pH was adjusted to $5.0 (\pm 0.2)$ by using 0.1 M HNO_3 or 0.1 M NaOH . For all sorption experiments, 100 mg biochar was added to 25 mL of Pb solution and shaken at $20 (\pm 2)^\circ\text{C}$ using an orbital shaker (KS 501 digital, IKATM, USA) at 180 rpm. All experiments were conducted in triplicate and the average values are reported. Additional analyses were performed when variations over 10% were observed. Samples were filtered through Whatman polyethersulfone syringe filters ($0.2 \mu\text{m}$) and analyzed by MP-AES (Agilent 4100, Agilent Technologies Inc., USA) at $\lambda = 405.781 \text{ nm}$ to quantify the remaining Pb concentration in solution.

Adsorption kinetic tests for Pb sorption onto raw and chemically-modified biochars from semi-continuous washing conditions (*i.e.* MSW^{sem} , $\text{MSW-H}_2\text{O}_2^{\text{sem}}$, $\text{MSW-KOH}^{\text{sem}}$, SS^{sem} , $\text{SS-H}_2\text{O}_2^{\text{sem}}$ and $\text{SS-KOH}^{\text{sem}}$) were performed to determine the time required to reach sorption equilibrium and the sorption kinetic constants using pseudo-first-order (PFO) and pseudo-second-order (PSO) models (kinetic equations are presented in Supplementary Information). These experiments were carried out with 100 mg L^{-1} Pb initial concentration, samples being collected after 10 min, 20 min, 30 min, 1 h, 2 h, 5 h, 7 h and 24 h of stirring.

Adsorption isotherms were performed with initial Pb concentrations between 10 and 1000 mg L^{-1} . Two common adsorption isotherm models (Langmuir and Freundlich) were used to fit the experimental data. The details of these adsorption isotherm equations are provided in the Supplementary Information.

3. Results and discussion

3.1. Characterization of raw and chemically modified biochars

The pH of suspensions of the raw and modified biochars is given in Table 1. A higher pH of the biochar compared to the raw feedstock was observed on both the organic fraction of municipal solid waste and sewage sludge digestate samples. The pH of MSW^{sem} and SS^{sem} was 8.9 and 6.5, respectively. This can be due to the presence of alkali compound (*i.e.* calcite) in the organic fraction of municipal solid waste biochar, while this component was not detected in sewage sludge digestate derived biochars (Fig. 1S). Chemical modification with KOH induced a significant shift to higher pH values, while a marginal pH variation was observed after H₂O₂ treatment (Table 2).

Table 1 shows the content of Ca, Mg, Na and K contained in the raw organic digestates (*i.e.* RMSW and RSS) and the derived biochars (*i.e.* MSW^{sem} and SS^{sem}). It was noticed that higher cationic macroelements were found in MSW^{sem} compared to SS^{sem}, particularly for Ca which was almost 4-fold higher in the former than in the latter (Table 1). In addition, the chemical characteristics such as ash and metal(loid) composition of RMSW, MSW^{sem}, RSS and SS^{sem} are reported in Table S2. The XRD characterization demonstrates kaolinite, quartz and calcite were present in the biochars (Fig. S1). The presence of these mineral phases on the biochar surface could facilitate the sorption of metals (Al-Degs et al., 2006; Jiang et al., 2009). Additionally, biochar displays the presence of Al, Fe and Mn (Table 1) that could be partially in metal oxide form, *i.e.* Al₂O₃, Fe₂O₃ and MnO. Thus, this could also promote interaction between the metal ions and biochar (Agrafioti et al., 2014; Wang et al., 2015).

FTIR spectra of MSW^{sem} and SS^{sem} show variations of the surface functional groups according to different biochar types (Fig. S2(a)). After alkali modification, stronger absorbance peaks corresponding to vibration of O–H functional groups (3425 cm⁻¹), –CH₃

stretching of long chain aliphatic groups (2924 cm^{-1}) and vibration of the C–C skeleton and C–O stretching (1033 cm^{-1}) were found, especially on SS-KOH^{sem} (Fig. S2(b)). Similar observations were reported by Petrovic et al. (2016) after alkali treatment of biochars. In addition, the FTIR spectra became more intense after H₂O₂ modification, particularly at 1640 cm^{-1} which is assigned to the vibrations of C=O bands (ester) (Fig. S2(b)). Such surface functional groups can take part in the sorption mechanisms for metals (Chen et al., 2011; Pituello et al., 2014).

From Table 2, the BET specific surface areas of SS-H₂O₂^{sem} and SS-KOH^{sem} were 3.7 and $3.0\text{ m}^2\text{ g}^{-1}$, respectively. These values increased after continuous washing with ultrapure water, probably due to the elimination of the ash content or organic matter from biochar pore sites.

3.2. Effect of biochar washing after chemical modification

After several batch-washings (semi-continuous mode) of KOH and H₂O₂-treated sewage sludge biochar, a subsequent column washing (continuous mode) was performed to highlight possible releases of organic or inorganic compounds from the biochar.

Fig. 1(a) and 1(b) represent the evolution of pH and conductivity of SS-KOH^{sem} and SS-H₂O₂^{sem}, respectively, along the column washing time. During the initial stage of washing (0–5 h), increases in pH were noticed for both KOH and H₂O₂-treated sewage sludge biochar. However, after 23 h, the pH of SS-KOH^{sem} started to decrease steadily before it became stable at pH 8.4 (after 64 h). The pH values remained almost unchanged at $6.5 (\pm 0.1)$ for SS-H₂O₂^{sem} beyond 23 h. On the other hand, decreasing trends of conductivities throughout the manipulation were observed on both chemically-modified biochars (Fig. 1 (a, b)). The values dramatically dropped from $309\text{--}391\text{ }\mu\text{S cm}^{-1}$ (at the beginning) to 4–6 μS

cm^{-1} (at the end of operation), which was comparable to the conductivity of ultrapure water from the inlet flow ($\sim 3 \mu\text{S cm}^{-1}$).

Fig. 1(c) and 1(d) show the changes of phosphate, inorganic carbon and dissolved organic matter released from SS-KOH^{sem} and SS-H₂O₂^{sem}, respectively, during column washing. The reduction of the PO₄³⁻, CO₃²⁻, HCO₃⁻ and DOC concentrations occurred continuously throughout the period of biochar washing (Fig. 1 (c, d)). Such evolutions are consistent with the conductivity trends (Fig. 1(a, b, c, d)). For instance, the high release of PO₄³⁻ (55 mg L⁻¹), CO₃²⁻ (99 mg L⁻¹) and HCO₃⁻ (1418 mg L⁻¹) from KOH-treated biochar was related to the high conductivity (391 $\mu\text{S cm}^{-1}$) (Fig. 1(a, c)) at the initial washing stage. Declining trends of the released compounds were observed along the lower conductivity level (Fig. 1(a, c)). Similarly, SS-H₂O₂^{sem} showed the same behavior as SS-KOH^{sem}, but with much lower PO₄³⁻, CO₃²⁻, HCO₃⁻ and DOC concentrations (Fig. 1 (b, d)). By comparing KOH and H₂O₂ treatment, it appears that after KOH treatment the biochar released more organic compounds, PO₄³⁻ and CO₃²⁻ /HCO₃⁻ compared to the H₂O₂ treatment. The DOC released was about 10-fold higher for SS-KOH^{sem} than for SS-H₂O₂^{sem} (at 1 h) (Fig. 1(c, d)). This is likely due to the property of KOH to modify the biochar surface. A similar behavior could be observed on the FTIR spectra, with a significant increase of transmittance for SS biochar treated with KOH (Fig. S2(b, c)).

These results clearly illustrate that a semi-continuous washing of chemically-treated biochar up to a stable pH was not sufficient to prevent the release of organic matter and ions. Indeed, in the batch reactor an equilibrium of released elements was achieved and the pH is usually used as an indicator for biochar washing (Huang et al., 2017; Regmi et al., 2012; Wu et al., 2017). However, to directly control the release of ions such as PO₄³⁻ and HCO₃⁻ /CO₃²⁻ from the biochar, conductivity is proposed as a more accurate parameter

rather than the pH. Therefore, a continuous washing with conductivity monitoring is recommended.

3.3. Adsorption kinetics

Fig. 2 shows the effect of contact time on the Pb removal capacity of MSW^{sem} , $\text{MSW-H}_2\text{O}_2^{\text{sem}}$, $\text{MSW-KOH}^{\text{sem}}$, SS^{sem} , $\text{SS-H}_2\text{O}_2^{\text{sem}}$ and $\text{SS-KOH}^{\text{sem}}$. The time required to reach the equilibrium state was different for each biochar type (Fig. 2). For sewage sludge based biochars, the equilibrium time was achieved after 5 h for raw SS^{sem} , 7 h for $\text{SS-H}_2\text{O}_2^{\text{sem}}$ and 2 h for $\text{SS-KOH}^{\text{sem}}$, while MSW-based biochars showed faster kinetics compared to SS biochars in which the equilibrium time was reached within 5 h for MSW^{sem} , 2 h for $\text{MSW-KOH}^{\text{sem}}$ and 1 h for $\text{MSW-H}_2\text{O}_2^{\text{sem}}$.

The data of the kinetic experiments were fitted using pseudo-first-order and pseudo-second-order equations. The corresponding kinetic parameters are given in Table S3. The pseudo-second order kinetic model was the most suitable to fit the experimental data for all biochars (Table S3). Considering the parameter k_2 , it could be concluded that $\text{MSW-H}_2\text{O}_2^{\text{sem}}$ exhibited the fastest kinetic rate followed by $\text{MSW-KOH}^{\text{sem}}$, $\text{SS-KOH}^{\text{sem}}$, MSW^{sem} , SS^{sem} and $\text{SS-H}_2\text{O}_2^{\text{sem}}$ (Table S3). In addition, the equilibrium adsorption capacities determined by the second order model (Q_e) were in agreement with the experimental ones ($Q_{e,\text{exp}}$) (Table S3).

Comparison of the different chemical modifications for biochar indicated that the alkali treatment (KOH) could induce a faster Pb removal rate, especially for the organic fraction of municipal solid waste (MSW) biochar. This was supported by a previous study from Regmi et al. (2012) on a switchgrass biochar treated with alkali reagent. In contrast, biochar modified with an oxidizing agent (H_2O_2) may not always increase the kinetic rate for Pb sorption. In this case, $\text{SS-H}_2\text{O}_2^{\text{sem}}$ reached equilibrium slightly slower than SS^{sem} .

Different kinetic rates for Pb adsorption were observed when comparing SS^{sem} and MSW^{sem}, the former requiring a longer time to reach sorption equilibrium. This was mainly due to differences in biochar properties resulting from the different origin of these biochars. FTIR spectra show stronger peaks of O-containing functional groups in MSW^{sem} compared to SS^{sem} especially at 1033 cm⁻¹ (Fig. S2(a)), which could induce a faster kinetic rate for metals (Bogusz et al., 2017). In addition, MSW^{sem} biochar contained calcite on its surface (Fig. S1(a)) and had higher cationic macroelements (*i.e.* Ca, K, Mg and Na) content than SS^{sem} biochar (Table 1) which could promote cationic metal (*i.e.* Pb) binding onto MSW^{sem} biochar. This is consistent with the study of Zhang et al. (2017) on the use of celery biochars with high amounts of alkaline minerals for cationic metal removal from aqueous solutions. However, the physical properties of biochar like porosity and specific surface area should be also considered as they play a role during the adsorption process.

3.4. Adsorption isotherms

Fig. 3(a) and 3(b) show the adsorption isotherms for Pb by semi-continuous washed SS^{sem}, SS-H₂O₂^{sem}, SS-KOH^{sem} and by MSW^{sem}, MSW-H₂O₂^{sem} and MSW-KOH^{sem}, respectively. Table 3 presents the fitting parameters of the Langmuir and Freundlich isotherm models. All experimental data could be well-described by the Langmuir adsorption isotherms model ($R^2 > 0.98$), except for SS-KOH^{sem}.

The results from Fig. 3(a) demonstrate that chemical treatment of biochar could enhance the Pb sorption capacity from 6.5 mg g⁻¹ on SS^{sem} to 25.1 mg g⁻¹ on SS-H₂O₂^{sem}. However, it was completely different for SS-KOH^{sem} due to unexpected low Pb adsorption capacities at low equilibrium Pb concentration (0–50 mg L⁻¹). As a result, the Langmuir model failed to describe the behavior of this sorption curve. One hypothesis is that a large amount of organic matter released from SS-KOH^{sem} (Fig. 1(c)) inhibits the Pb sorption onto

the biochar by forming soluble Pb-ligand complexes, resulting in lower Q_e values at the low C_e range (0–50 mg L⁻¹).

Fig. 3(b) shows that the Pb sorption capability was improved by KOH and H₂O₂ treatment of MSW biochar. It increased from 72.9 mg g⁻¹ for MSW^{sem} to 90.0 mg g⁻¹ and 106.3 mg g⁻¹ for MSW-H₂O₂^{sem} and MSW-KOH^{sem}, respectively. This implies that chemical treatment could be effectively used to promote Pb sorption onto the organic fraction of municipal solid waste-based biochar.

Fig. 4(a) shows the Pb adsorption isotherms on sewage sludge digestate-based biochars fitted with the Langmuir model (except KOH^{sem} due to non-fitting). Fig. 4(b) and 4(c) compare the adsorption isotherms obtained for two different washing systems: batch semi-continuous versus batch followed by column continuous washing. From Fig. 4(b), a significant enhancement of Pb sorption by KOH^{con} (continuous washed) was observed compared to KOH^{sem} (semi-continuous washed) particularly at low C_e (0–50 mg L⁻¹), highlighting the importance of biochar washing after chemical treatment. These results are consistent with the hypothesis of Pb sorption inhibition due to the formation of soluble complexes with organic matter released by the biochar. Such compounds were removed during the subsequent column washing, leading to a higher sorption capacity for KOH^{con} compared to KOH^{sem}, especially at low Pb equilibrium concentrations. In addition, the Langmuir adsorption model was then able to fit with experimental data of KOH^{con} (Table 3). However, no significant differences in Pb sorption capacities between KOH^{sem} and KOH^{con} were observed at higher C_e (400–1000 mg L⁻¹) (Fig. 4(a)). This implies that the presence of organic matter in aqueous solutions significantly affects the Pb sorption onto biochar only at low Pb ion concentrations, especially <50 mg L⁻¹.

In contrast, similar adsorption capacities for Pb by both H₂O₂^{sem} and H₂O₂^{con} were achieved, even at low Pb equilibrium concentrations (0–30 mg L⁻¹, Fig. 4(c)). This is

because H_2O_2 treatment induced a small release of inorganic and organic matter from the modified biochar. As a result, batch washing was sufficient and no improvement was obtained with the subsequent column washing.

Fig. 4(d) and 4(e) compare the adsorption isotherms at low C_e for Pb by H_2O_2 and KOH treated sewage sludge biochars on semi-continuous washing and continuous washing, respectively. The conclusions totally differ according to the washing procedure: the semi-continuous washing indicates that sorption is more important after H_2O_2 (Fig. 4(d)), whereas the continuous washing leads to the opposite conclusion (Fig. 4(e)). This is the consequence of the uncompleted efficiency of batch washing to remove the released compounds for biochar after KOH treatment.

Considering the maximal sorption capacity (Q_m) of each biochar (Table 3), chemical treatments of biochar with KOH and H_2O_2 show an improved Pb sorption capacity, particularly on sewage sludge digestate biochar. Results show an enhanced Q_m for Pb by almost 2-fold for SS- $\text{H}_2\text{O}_2^{\text{con}}$ and by 12-fold for SS-KOH $^{\text{con}}$ with respect to the unmodified SS biochar. The use of KOH for chemical treatment thus appears more efficient than H_2O_2 . However, a proper biochar washing procedure after chemical treatment is highly required to prevent the altered isotherm shape.

3.5. Possible Pb sorption mechanisms

Previous studies have illustrated the correlation of sorption for Cu^{2+} , Cd^{2+} and Pb^{2+} with the oxygen-contained functional groups obtained from FTIR analysis (Petrovic et al., 2016; Regmi et al., 2012). The interactions between Pb and available surface functional groups on biochar can occur through surface complexation. In addition, possible cation exchange may take place. This is consistent with the observed release of Ca^{2+} and Mg^{2+} in solution after Pb sorption (Fig. 5).

Fig. 5(a) compares the cations (Ca^{2+} and Mg^{2+}) released by KOH-modified sewage sludge biochars from semi-continuous and continuous washing. The results show that the concentration of Ca^{2+} and Mg^{2+} released from SS-KOH^{sem} was relatively low (<3 mg L⁻¹) at initial Pb concentrations between 0–203 mg L⁻¹. This was in correlation to a low sorption capacity for Pb by SS-KOH^{sem} (see section 3.4). In contrast, a huge release of Ca^{2+} and Mg^{2+} by SS-KOH^{con} was observed at adsorption equilibrium (Fig. 5(a)). The released Ca^{2+} and Mg^{2+} from this biochar was related to the amount of Pb adsorbed onto the biochar surface (on molecular mass basis) (Fig. 5(b)). These findings are in accordance with previous studies of biochars produced from grape pomace and water hyacinth for Pb and Cd removal, respectively (Petrovic et al., 2016; Zhang et al., 2015).

Moreover, the characterization of biochar shows the presence of a mineral phase that could also be involved in Pb sorption (Fig. S1). Nevertheless, previous links between the release of cations from biochar and the Pb sorption capacity show that sorption of Pb by the mineral phase in the biochar is not the main mechanism involved in sorption. In addition, Pb precipitation onto sludge biochar may contribute to the sorption mechanism. The results from the simulation shows that at initial Pb concentrations of 10 and 970 mg L⁻¹ (Fig. S3), Pb precipitation onto biochar will likely occur when the final pH values are above 6.0 and above 5.0, respectively. Since the final pH in the solutions of both SS-KOH^{sem} and MSW-KOH^{sem} were above these values, Pb precipitation partly occurred on both biochar types during the sorption experiments.

3.6. Practical implications

The conversion of organic digested sludge obtained from wastewater treatment plants through pyrolysis is considered as a promising approach for sludge management. This corresponds to a huge reduction of the sludge quantity as well as a decrease of metal mobility

in the sludge. It also promotes the environmental sustainability strategy due to recycling of the organic wastes and adding more value to the obtained products (*i.e.* biochar).

Chemical modification of biochar has been suggested as an economical technique to improve the sorption performance for Pb. From this study, treatment of biochar with chemical reagents affected the sorption kinetics for Pb. In this case, KOH could induce faster Pb removal rates compared to the unmodified biochars, while it was not systematic for biochars treated with H₂O₂. Furthermore, the chemically-modified biochars reveal a significant Pb sorption enhancement, but with a caution on proper-washed biochar especially with KOH treatment. Indeed, we observed that this treatment led to an inhibition of Pb sorption at low Pb initial concentration linked to the release of complexing compounds (*e.g.* phosphate, (bi)carbonate and organic matter). Thus, a sufficient biochar washing is required to remove these compounds prior to practical applications to ensure an improvement of the Pb sorption features and avoid the contamination of water bodies by the released products. Future research on the effect of biochar washing after chemical treatment is required to better understand the role of released organic compounds and other alkali anion ions on Pb sorption by sludge-based biochar.

4. Conclusions

This study demonstrated the capability of raw digested sludge biochars and chemically-modified biochars in Pb removal from water through adsorption kinetic and isotherm studies. Lead sorption data could be well-described by the Langmuir isotherm model and followed the pseudo-second-order kinetic model. The KOH treatment was found more efficient than the H₂O₂ treatment to improve Pb sorption, with an improvement of both the sorption kinetics and capacity. In the case of sewage sludge biochar, the sorption capacity was about 2-fold and 10-fold higher after H₂O₂ and KOH treatment, respectively. However,

special attention should be paid to the washing procedure after chemical modification to avoid an inhibition of metal sorption due to a significant release of soluble compounds from an improperly washed modified biochar.

Acknowledgements

Patrice Fondanèche is acknowledged for technical assistance with the Pb measurement. This research project has received funding from the European Union's Horizon 2020 research and innovation programme under the Marie Skłodowska-Curie grant agreement N° 643071.

References

- Afnor, 1997a. Qualité de l'eau. Tome 2. Lignes directrices pour le dosage du carbone organique total (TOC) et carbone organique dissous (COD). Norme EN 1484, sixth ed. France.
- Afnor, 1997b. Qualité de l'eau. Tome 3. Dosage du phosphore. Dosage spectrométrique à l'acide du molybdate d'ammonium. Norme EN 1189, sixth ed. France.
- Afnor, 1996. Qualité de l'eau. Tome 2. Détermination de l'alcalinité. Norme EN ISO 9963-1, sixth ed. France.
- Agrafioti, E., Kalderis, D., Diamadopoulos, E., 2014. Arsenic and chromium removal from water using biochars derived from rice husk, organic solid wastes and sewage sludge. *J. Environ. Manage.* 133, 309–314.
- Al-Degs, Y.S., El-Barghouthi, M.I., Issa, A.A., Khraisheh, M.A., Walker, G.M., 2006. Sorption of Zn(II), Pb(II), and Co(II) using natural sorbents: Equilibrium and kinetic studies. *Water Res.* 40, 2645–2658.
- Andrejkovicova, S., Sudagar, A., Rocha, J., Patinha, C., Hajjaji, W., Da Silva, E.F., Velosa,

- A., Rocha, F., 2016. The effect of natural zeolite on microstructure, mechanical and heavy metals adsorption properties of metakaolin based geopolymers. *Appl. Clay Sci.* 126, 141–152.
- Bogusz, A., Nowak, K., Stefaniuk, M., Dobrowolski, R., Oleszczuk, P., 2017. Synthesis of biochar from residues after biogas production with respect to cadmium and nickel removal from wastewater. *J. Environ. Manage.* 201, 268–276.
- Cechinel, M.A.P., Ulson De Souza, S.M.A.G., Ulson De Souza, A.A., 2014. Study of lead (II) adsorption onto activated carbon originating from cow bone. *J. Clean. Prod.* 65, 342–349.
- Chen, X., Chen, G., Chen, L., Chen, Y., Lehmann, J., McBride, M.B., Hay, A.G., 2011. Adsorption of copper and zinc by biochars produced from pyrolysis of hardwood and corn straw in aqueous solution. *Bioresour. Technol.* 102, 8877–8884.
- EPA., US, 1996. Acid digestion of sediments, sludges, and soils, revision 2, 1–12.
- Fan, S., Tang, J., Wang, Y., Li, H., Zhang, H., Tang, J., Wang, Z., Li, X., 2016. Biochar prepared from co-pyrolysis of municipal sewage sludge and tea waste for the adsorption of methylene blue from aqueous solutions: Kinetics, isotherm, thermodynamic and mechanism. *J. Mol. Liq.* 220, 432–441.
- Ho, S.H., Chen, Y., Yang, Z., Nagarajan, D., Chang, J.S., Ren, N., 2017. High-efficiency removal of lead from wastewater by biochar derived from anaerobic digestion sludge. *Bioresour. Technol.* 246, 142–149.
- Huang, H., Tang, J., Gao, K., He, R., Zhao, H., Werner, D., 2017. Characterization of KOH modified biochars from different pyrolysis temperatures and enhanced adsorption of antibiotics. *RSC Adv.* 7, 14640–14648.
- Inyang, M., Gao, B., Yao, Y., Xue, Y., Zimmerman, A.R., Pullammanappallil, P., Cao, X., 2012. Removal of heavy metals from aqueous solution by biochars derived from

- anaerobically digested biomass. *Bioresour. Technol.* 110, 50–56.
- Inyang, M.I., Gao, B., Yao, Y., Xue, Y., Zimmerman, A., Mosa, A., Pullammanappallil, P., Ok, Y.S., Cao, X., 2016. A review of biochar as a low-cost adsorbent for aqueous heavy metal removal. *Crit. Rev. Environ. Sci. Technol.* 4, 406–433.
- Jiang, M., Wang, Q., Jin, X., Chen, Z., 2009. Removal of Pb(II) from aqueous solution using modified and unmodified kaolinite clay. *J. Hazard. Mater.* 170, 332–339.
- Jin, H., Capareda, S., Chang, Z., Gao, J., Xu, Y., Zhang, J., 2014. Biochar pyrolytically produced from municipal solid wastes for aqueous As(V) removal: Adsorption property and its improvement with KOH activation. *Bioresour. Technol.* 169, 622–629.
- Kaul, B., Sandhu, R.S., Depratt, C., Reyes, F., 1999. Follow-up screening of lead-poisoned children near an auto battery recycling plant, Haina, Dominican Republic. *Environ. Health Perspect.* 107, 917–920.
- Li, H., Dong, X., da Silva, E.B., de Oliveira, L.M., Chen, Y., Ma, L.Q., 2017. Mechanisms of metal sorption by biochars: Biochar characteristics and modifications. *Chemosphere* 178, 466–478.
- Li, J., Li, Y., Wu, Y., Zheng, M., 2014. A comparison of biochars from lignin, cellulose and wood as the sorbent to an aromatic pollutant. *J. Hazard. Mater.* 280, 450–457.
- Lin, Y., Munroe, P., Joseph, S., Henderson, R., Ziolkowski, A., 2012. Water extractable organic carbon in untreated and chemical treated biochars. *Chemosphere* 87, 151–157.
- Liou, T.H., Wu, S.J., 2009. Characteristics of microporous/mesoporous carbons prepared from rice husk under base- and acid-treated conditions. *J. Hazard. Mater.* 171, 693–703.
- Liu, P., Liu, W.J., Jiang, H., Chen, J.J., Li, W.W., Yu, H.Q., 2012. Modification of bio-char derived from fast pyrolysis of biomass and its application in removal of tetracycline from aqueous solution. *Bioresour. Technol.* 121, 235–240.
- Liu, Z., Zhang, F.S., 2009. Removal of lead from water using biochars prepared from

- hydrothermal liquefaction of biomass. *J. Hazard. Mater.* 167, 933–939.
- Lu, H., Zhang, W., Yang, Y., Huang, X., Wang, S., Qiu, R., 2012. Relative distribution of Pb²⁺ sorption mechanisms by sludge-derived biochar. *Water Res.* 46, 854–862.
- Mohan, D., Sarswat, A., Ok, Y.S., Pittman, C.U., 2014. Organic and inorganic contaminants removal from water with biochar, a renewable, low cost and sustainable adsorbent – A critical review. *Bioresour. Technol.* 160, 191–202.
- Petrovic, J.T., Stojanovic, M.D., Milojkovic, J. V., Petrovic, M.S., Sostaric, T.D., Lausevic, M.D., Mihajlovic, M.L., 2016. Alkali modified hydrochar of grape pomace as a perspective adsorbent of Pb²⁺ from aqueous solution. *J. Environ. Manage.* 182, 292–300.
- Pituello, C., Francioso, O., Simonetti, G., Pisi, A., Torreggiani, A., Berti, A., Morari, F., 2014. Characterization of chemical–physical, structural and morphological properties of biochars from biowastes produced at different temperatures. *J. Soils Sediments* 15, 792–804.
- Rajapaksha, A.U., Chen, S.S., Tsang, D.C.W., Zhang, M., Vithanage, M., Mandal, S., Gao, B., Bolan, N.S., Ok, Y.S., 2016. Engineered/designer biochar for contaminant removal/immobilization from soil and water: Potential and implication of biochar modification. *Chemosphere* 148, 276–291.
- Regmi, P., Garcia Moscoso, J.L., Kumar, S., Cao, X., Mao, J., Schafran, G., 2012. Removal of copper and cadmium from aqueous solution using switchgrass biochar produced via hydrothermal carbonization process. *J. Environ. Manage.* 109, 61–69.
- Saifullah, Dahlawi, S., Naeem, A., Rengel, Z., Naidu, R., 2018. Biochar application for the remediation of salt-affected soils: Challenges and opportunities. *Sci. Total Environ.* 625, 320–335.
- Sizmur, T., Fresno, T., Akgül, G., Frost, H., Moreno Jiménez, E., 2017. Biochar modification to enhance sorption of inorganics from water. *Bioresour. Technol.* 246, 34–47.

- Tóth, G., Hermann, T., Silva, M.R. Da, Montanarella, L., 2016. Heavy metals in agricultural soils of the European Union with implications for food safety. *Environemtal Int.* 88, 299–309.
- Wang, S., Gao, B., Li, Y., Mosa, A., Zimmerman, A.R., Ma, L.Q., Harris, W.G., Migliaccio, K.W., 2015. Manganese oxide-modified biochars: Preparation, characterization, and sorption of arsenate and lead. *Bioresour. Technol.* 181, 13–17.
- Wang, Y., Liu, R., 2018. H_2O_2 treatment enhanced the heavy metals removal by manure biochar in aqueous solutions. *Sci. Total Environ.* 628–629, 1139–1148.
- Wu, W., Li, J., Lan, T., Müller, K., Khan, N., Chen, X., Xu, S., Zheng, L., Chu, Y., Li, J., Yuan, G., Wang, H., 2017. Unraveling sorption of lead in aqueous solutions by chemically modified biochar derived from coconut fiber: A microscopic and spectroscopic investigation. *Sci. Total Environ.* 576, 766–774.
- Xue, Y., Gao, B., Yao, Y., Inyang, M., Zhang, M., Zimmerman, A.R., Ro, K.S., 2012. Hydrogen peroxide modification enhances the ability of biochar (hydrochar) produced from hydrothermal carbonization of peanut hull to remove aqueous heavy metals: Batch and column tests. *Chem. Eng. J.* 200–202, 673–680.
- Zhang, F., Wang, X., Yin, D., Peng, B., Tan, C., Liu, Y., Tan, X., Wu, S., 2015. Efficiency and mechanisms of Cd removal from aqueous solution by biochar derived from water hyacinth (*Eichornia crassipes*). *J. Environ. Manage.* 153, 68–73.
- Zhang, T., Zhu, X., Shi, L., Li, J., Li, S., Lu, J., Li, Y., 2017. Efficient removal of lead from solution by celery-derived biochars rich in alkaline minerals. *Bioresour. Technol.* 235, 185–192.
- Zhang, W., Mao, S., Chen, H., Huang, L., Qiu, R., 2013. Pb(II) and Cr(VI) sorption by biochars pyrolyzed from the municipal wastewater sludge under different heating conditions. *Bioresour. Technol.* 147, 545–552.

Zielińska, A., Oleszczuk, P., Charmas, B., Skubiszewska-Zięba, J., Pasieczna-Patkowska, S.,
2015. Effect of sewage sludge properties on the biochar characteristic. *J. Anal. Appl. Pyrolysis* 112, 201–213.

Figures

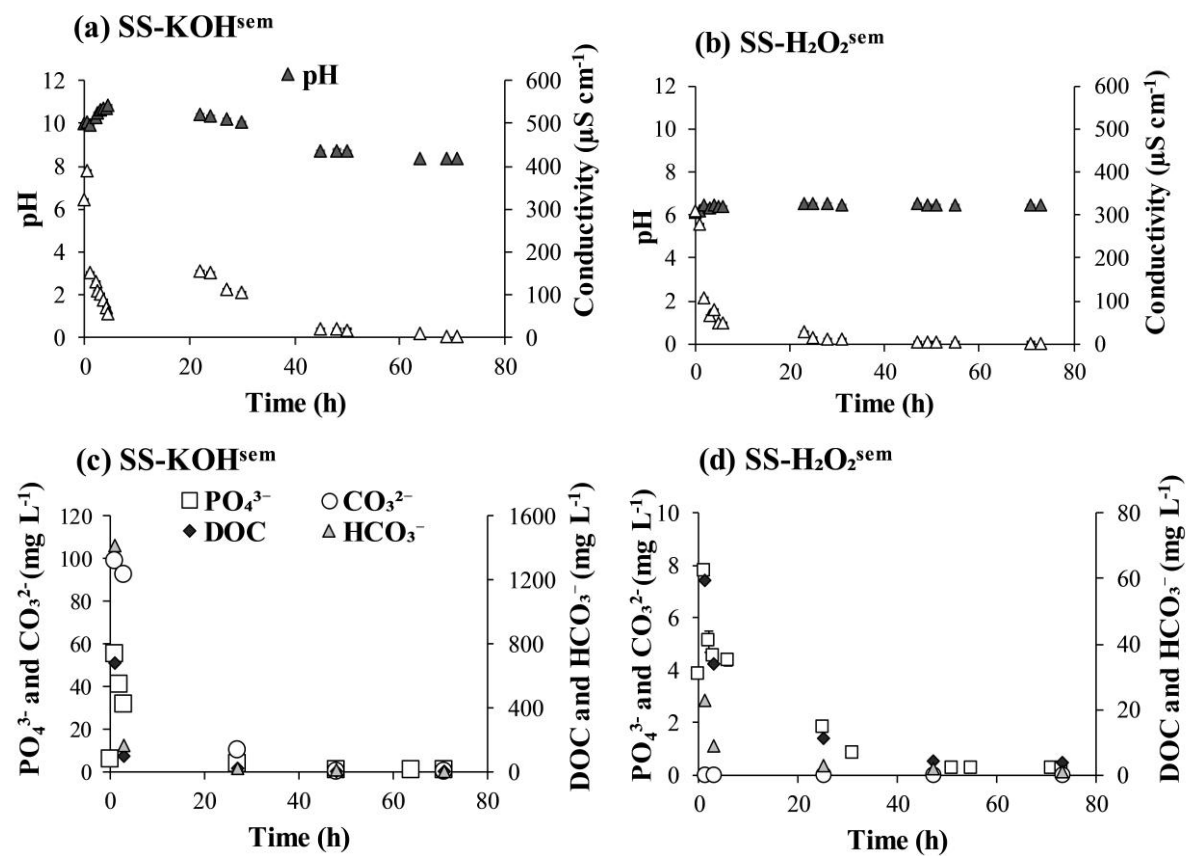


Fig. 1. Evolution of pH and conductivity during continuous washing of SS-KOH^{sem} (a) and SS-H₂O₂^{sem} (b), and concentration profile of phosphate, (bi)carbonate and dissolved organic carbon (DOC) along continuous washing of SS-KOH^{sem} (c) and SS-H₂O₂^{sem} (d).

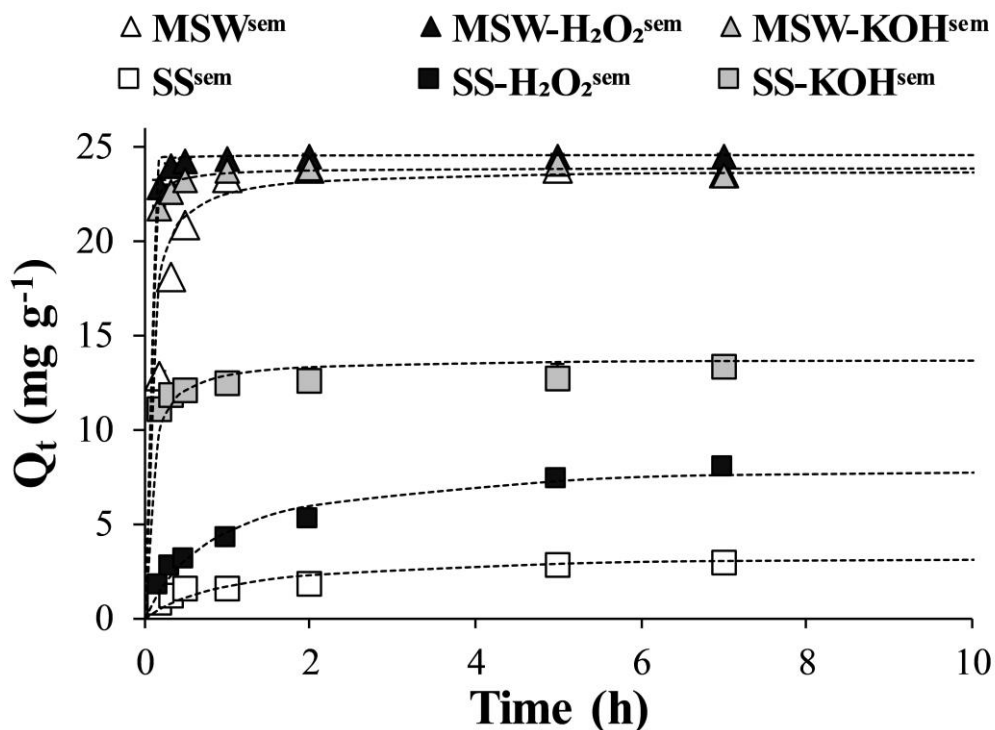


Fig. 2. Adsorption kinetics for Pb by semi-continuous washed MSW^{sem} , $\text{MSW-H}_2\text{O}_2^{\text{sem}}$, $\text{MSW-KOH}^{\text{sem}}$, SS^{sem} , $\text{SS-H}_2\text{O}_2^{\text{sem}}$ and $\text{SS-KOH}^{\text{sem}}$ at different contact times at an initial solution pH of 5 and initial Pb concentration of 100 mg L^{-1} fitted with the pseudo-second order kinetic model.

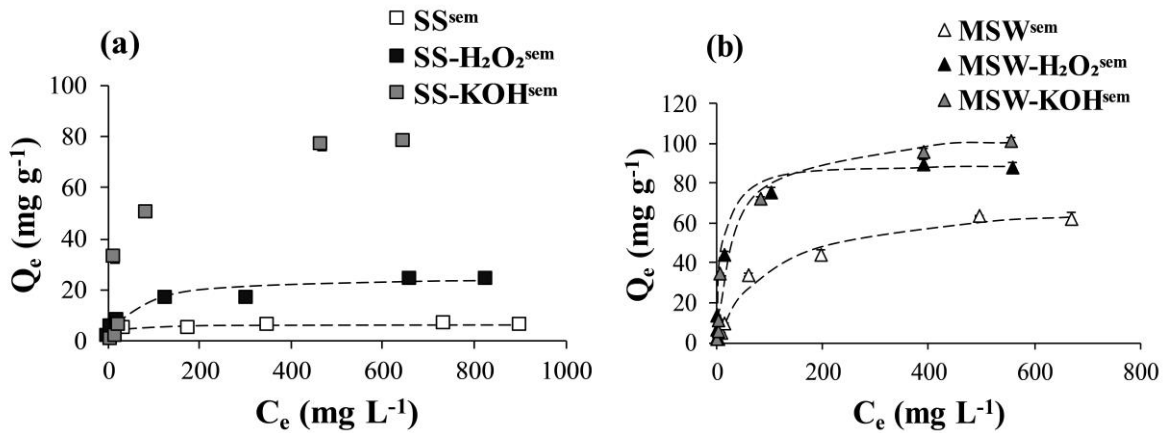


Fig. 3. Adsorption isotherms for Pb by semi-continuous washed SS^{sem} , $SS\text{-H}_2\text{O}_2^{\text{sem}}$ and $SS\text{-KOH}^{\text{sem}}$ (a) and by MSW^{sem} , $MSW\text{-H}_2\text{O}_2^{\text{sem}}$ and $MSW\text{-KOH}^{\text{sem}}$ (b) at different equilibrium Pb(II) concentrations at an initial solution pH of 5 fitted with the Langmuir model (except $SS\text{-KOH}^{\text{sem}}$ due to non-fitting).

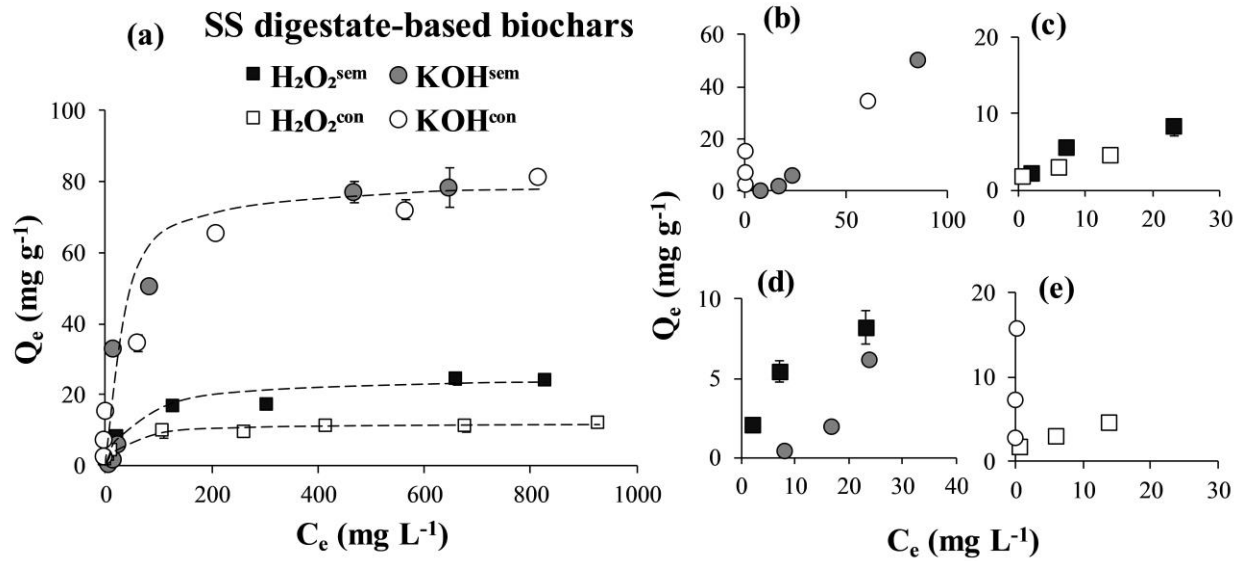


Fig. 4. Comparison of the Pb adsorption isotherms on sewage sludge digestate-based biochars with different washing modes fitted with the Langmuir model (except KOH^{sem} due to non-fitting) (a). Figure (b) to (e) are zooms of C_e at low concentration ranges ($< 100 \text{ mg L}^{-1}$); semi-continuous washed KOH^{sem} versus continuous washed KOH^{con} (b), $\text{H}_2\text{O}_2^{\text{sem}}$ versus $\text{H}_2\text{O}_2^{\text{con}}$ (c), and with different chemical treatments; KOH^{sem} versus $\text{H}_2\text{O}_2^{\text{sem}}$ (d), and KOH^{con} versus $\text{H}_2\text{O}_2^{\text{con}}$ (e).

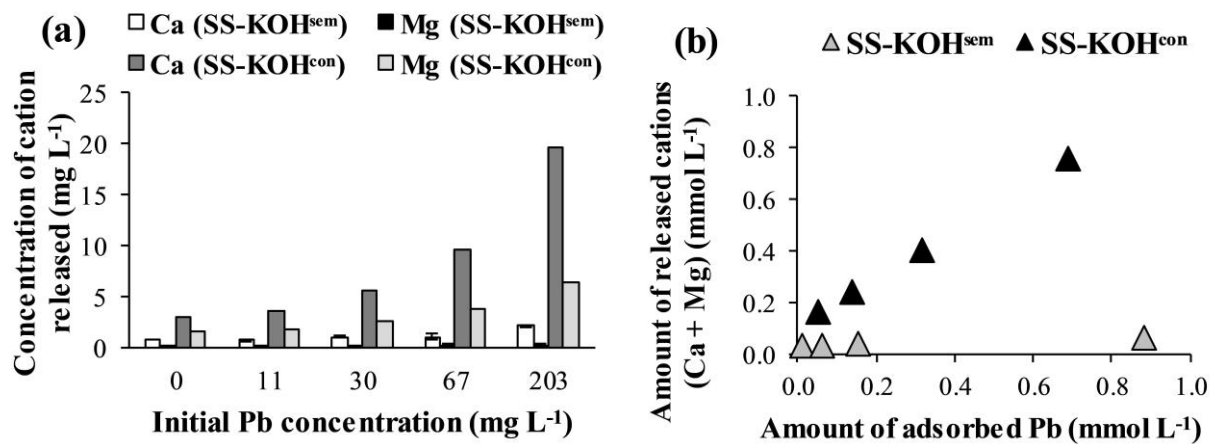


Fig. 5. Comparison of Ca^{2+} and Mg^{2+} released by $\text{SS-KOH}^{\text{sem}}$ (semi-continuous washed) and $\text{SS-KOH}^{\text{con}}$ (continuous washed) (a), and the amount of adsorbed Pb versus the summation of the released cations (Ca^{2+} and Mg^{2+}) at Pb adsorption equilibrium (b).

Tables

Table 1

The pH and concentrations of Ca, K, Mg, Na, Al, Fe and Mn in the raw organic fraction of municipal solid waste digestate (RMSW), its derived biochar (MSW^{sem}) with semi-continuous washing, raw sewage sludge digestate (RSS) and its derived biochar (SS^{sem}) with semi-continuous washing.

Biochar	pH in water	Ca (g kg ⁻¹)	K (g kg ⁻¹)	Mg (g kg ⁻¹)	Na (g kg ⁻¹)	Al (g kg ⁻¹)	Fe (g kg ⁻¹)	Mn (mg kg ⁻¹)
RMSW	8.0 ± 0.1	89.2 ± 1.4	32.1 ± 0.3	7.3 ± 0.1	32.2 ± 0.2	17.6 ± 0.2	11.4 ± 0.1	322.9 ± 2.7
MSW^{sem}	8.9 ± 0.1	114.9 ± 0.4	21.8 ± 0.2	10.4 ± 0.1	31.9 ± 0.2	14.2 ± 0.1	16.1 ± 0.2	417.4 ± 2.9
RSS	6.0 ± 0.1	20.2 ± 0.3	3.6 ± 0.9	5.3 ± 0.1	4.2 ± 0.5	11.4 ± 0.4	66.0 ± 0.8	476.9 ± 6.3
SS^{sem}	6.5 ± 0.1	29.5 ± 0.4	4.4 ± 0.1	8.0 ± 0.1	4.6 ± 0.1	14.3 ± 0.2	65.7 ± 0.8	769.9 ± 8.0

Table 2

The pH and specific surface area of chemically-modified sewage sludge digestate biochar with semi-continuous washing (SS-H₂O₂^{sem} and SS-KOH^{sem}) and with continuous washing (SS-H₂O₂^{con} and SS-KOH^{con}).

Biochar	pH in water	S _{BET} ^a (m ² g ⁻¹)
SS-H ₂ O ₂ ^{sem}	6.2 ± 0.1	3.6 ± 0.1
SS-KOH ^{sem}	10.1 ± 0.1	3.0 ± 0.1
SS-H ₂ O ₂ ^{con}	6.5 ± 0.1	5.7 ± 0.1
SS-KOH ^{con}	8.4 ± 0.1	7.9 ± 0.1

^a S_{BET} refers to Brunauer–Emmett–Teller (BET) surface area of biochar.

Table 3

Effect of biochar modification (H_2O_2 and KOH) and biochar washing (semi-continuous and continuous) on the Pb adsorption capacity.

Biochar	Langmuir isotherm model			Freundlich isotherm model		
	Q_m^{a}	K_L^{b}	R^2	K_F^{c}	n	R^2
MSW ^{sem}	72.9	0.010	0.992	1.430	1.584	0.940
MSW- $\text{H}_2\text{O}_2^{\text{sem}}$	90.0	0.109	0.999	9.895	2.624	0.894
MSW-KOH ^{sem}	106.3	0.030	0.997	4.908	1.888	0.860
SS ^{sem}	6.5	0.069	0.994	2.136	5.646	0.782
SS- $\text{H}_2\text{O}_2^{\text{sem}}$	25.1	0.018	0.984	2.117	2.633	0.955
SS-KOH ^{sem}	151.5	0.001	0.293	1.201	1.472	0.566
SS- $\text{H}_2\text{O}_2^{\text{con}}$	12.0	0.034	0.993	1.952	3.527	0.967
SS-KOH ^{con}	80.6	0.037	0.987	12.406	3.462	0.926

^a Q_m refers to the unit of mg g^{-1}

^b K_L refers to the unit of L mg^{-1}

^c K_F refers to the unit of $(\text{mg g}^{-1})(\text{L mg}^{-1})^{1/n}$

Supplementary Information

Lead sorption by biochar produced from digestates: Consequences of chemical modification and washing

Suchanya Wongrod^{a,b,c}, Stéphane Simon^c, Gilles Guibaud^{c,*}, Piet N.L. Lens^b, Yoan Pechaud^a, David Huguenot^a, Eric D. van Hullebusch^{a,b}

^a Université Paris-Est, Laboratoire Géomatériaux et Environnement (EA 4508), UPEM, 77454, Marne-la-Vallée, France

^b IHE Delft Institute for Water Education, P.O. Box 3015, 2601 DA Delft, The Netherlands

^c Université de Limoges, PEIRENE-Groupement de Recherche Eau Sol Environnement (EA 7500), Faculté des Sciences et Techniques, 123 avenue Albert Thomas, 87060 Limoges, France

*Corresponding author: gilles.guibaud@unilim.fr

XRD and FTIR analysis

X-ray diffractometry (XRD) was employed to identify the crystalline structures presented in raw and modified biochars. The samples were grounded to less than 100 μm particle size and were characterized using a powder diffractometer (AXS D8, Bruker, Germany) with Cu K α radiation at 1.54 \AA wavelength, over the 2θ range from 10° to 32°, for 10 seconds per step, at 40 kV voltage and 40 mA current with a Solx (Si-Li) detector. The crystalline compounds present in biochar were identified by search-match software with reference from the American Mineralogist Crystal Structure Database.

Fourier transform infrared spectroscopy (FTIR) were recorded to identify the functional groups present on biochar surfaces. Each sample was mixed with KBr in a ratio of 1 mg sample (particle size 100 μm) per 200 mg KBr and the pellet was prepared by compression under vacuum (Jouraiphy et al., 2005). The analysis was performed using a Shimadzu IRAffinity-1 Spectrometer with a deuterated-triglycine sulfate (DTGS) detector. The number of scans was 12 with a resolution of 16 cm^{-1} and a frequency in a range from 4000 to 800 cm^{-1} .

XRD spectra of biochars

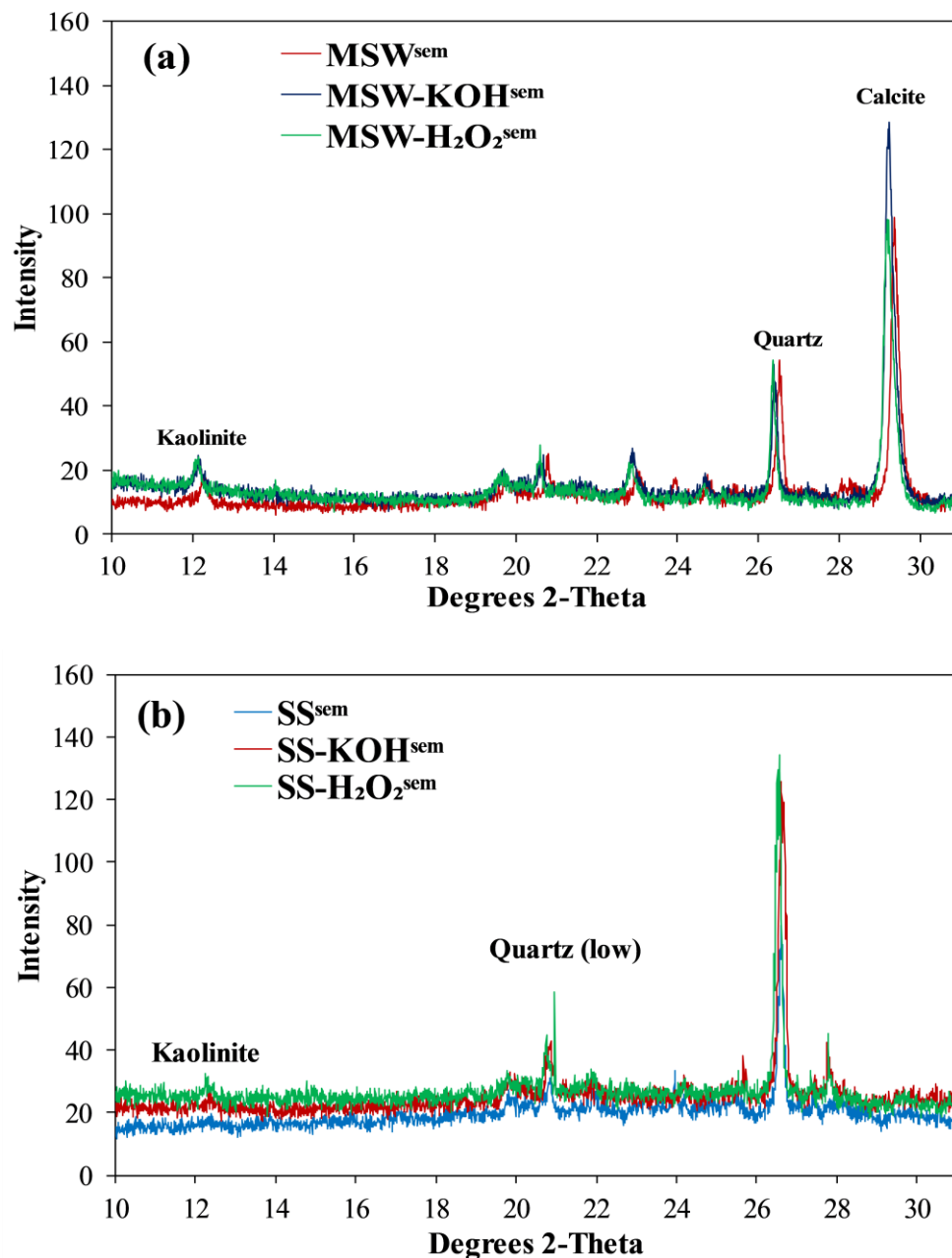


Fig. S1. XRD spectra of semi-continuous washed MSW^{sem} , $\text{MSW-KOH}^{\text{sem}}$ and $\text{MSW-H}_2\text{O}_2^{\text{sem}}$ (a) and SS^{sem} , $\text{SS-KOH}^{\text{sem}}$ and $\text{SS-H}_2\text{O}_2^{\text{sem}}$ (b).

XRD analysis showed that MSW^{sem} contained the crystalline structures of kaolinite ($\text{Al}_2\text{Si}_2\text{O}_5(\text{OH})_4$), quartz (SiO_2) and calcite (CaCO_3) at 2θ 12.38° , 26.68° and 29.51° ,

respectively (Fig. S1(a)). Similar trends were also found in its chemically-modified biochar with slight shifts on the XRD spectra. For instance, the XRD peak of CaCO_3 was shifted from 29.36° (MSW^{sem}) to 29.23° ($\text{MSW-KOH}^{\text{sem}}$) and 29.20° ($\text{MSW-H}_2\text{O}_2^{\text{sem}}$). On the other hand, only $\text{Al}_2\text{Si}_2\text{O}_5(\text{OH})_4$ and SiO_2 were detected in SS^{sem} , $\text{SS-KOH}^{\text{sem}}$ and $\text{SS-H}_2\text{O}_2^{\text{sem}}$ (Fig. S1(b)). The results showed no significant differences of XRD spectra between the raw and chemical treated sewage sludge biochars. Kaolinite and carbonates present in the biochar can be partly involved in adsorption of Pb onto the biochar surface.

FTIR spectra of biochars

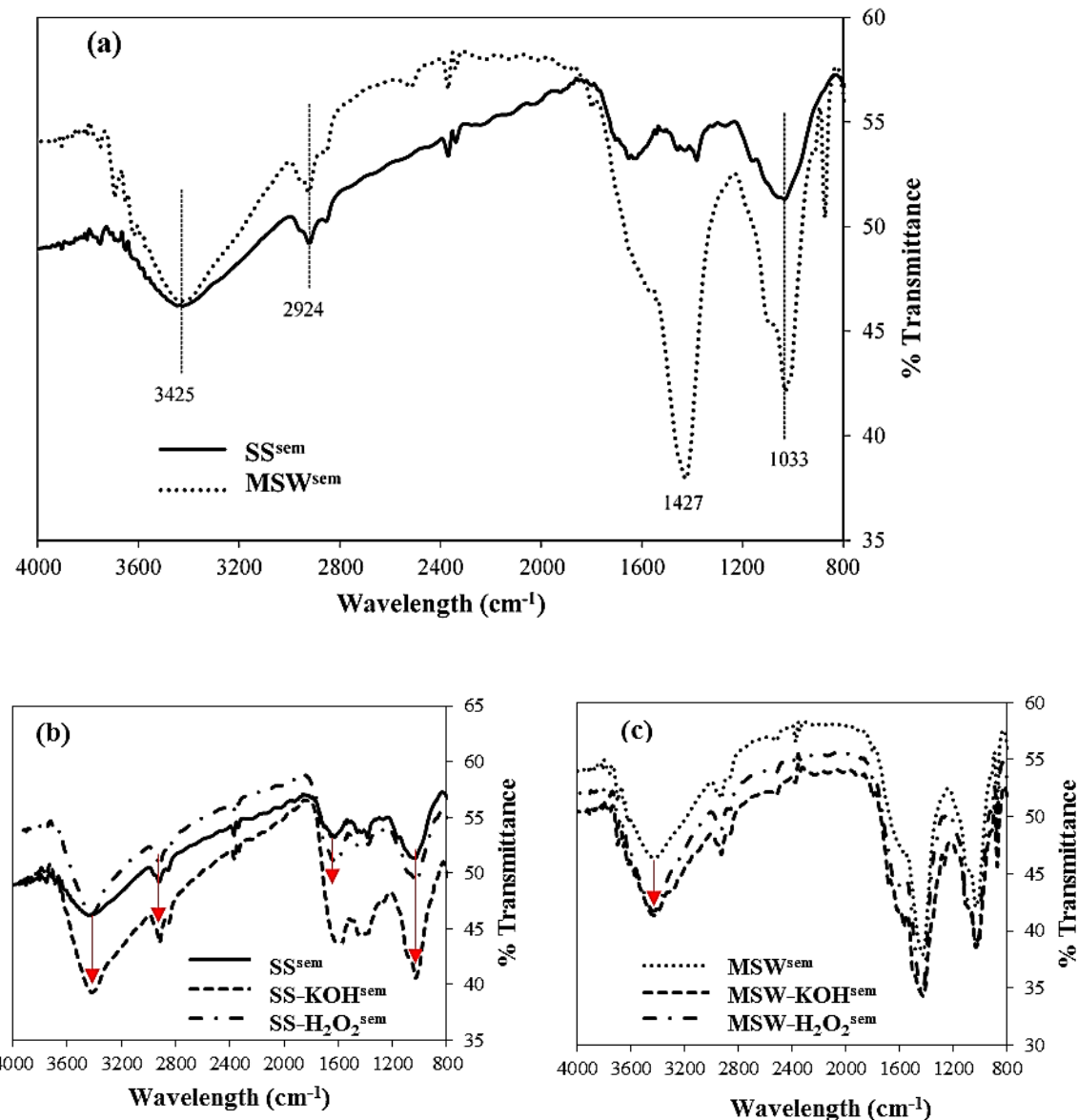


Fig. S2. Comparison of the FTIR spectra of semi-continuous washed SS^{sem} and MSW^{sem} (a), SS^{sem} , $\text{SS-KOH}^{\text{sem}}$, $\text{SS-H}_2\text{O}_2^{\text{sem}}$ (b), and MSW^{sem} , $\text{MSW-KOH}^{\text{sem}}$ and $\text{MSW-H}_2\text{O}_2^{\text{sem}}$ (c).

The peak band of 3425 cm^{-1} referred to the stretching vibration of O–H functional groups (H-bonded) of alcohols and phenols and was present in all biochars (Fig. S2(a)). The bands at 2924 cm^{-1} was due to the vibration of C–H stretching of long chain aliphatic groups (Chen et al., 2011) and was also found in all biochars (Fig. S2(a)). The bands of 1660–1600

cm^{-1} were assigned to the stretching vibrations of C=C and were observed only in SS^{sem} , $\text{SS-KOH}^{\text{sem}}$ and $\text{SS-H}_2\text{O}_2^{\text{sem}}$ (Fig. S2(b)). Since sewage sludge digestate is generally composed of cellulose, hemicellulose and lignin (Jouraiphy et al., 2005), thus the spectra of the amides band are broad bands of 1690 – 1640 cm^{-1} . The broad bands between 1442 – 1384 cm^{-1} was assigned to $-\text{CH}_2$ scissoring and were observed in raw and modified biochars from sewage sludge (Fig. S2(b)). A strong intensity of $-\text{CH}_2$ scissoring was found at a peak of 1427 cm^{-1} in MSW^{sem} , $\text{MSW-KOH}^{\text{sem}}$ and $\text{MSW-H}_2\text{O}_2^{\text{sem}}$ (Fig. S2(c)). The stretching of carboxylate groups and C–O of alcohols appeared in the sample between 1300 and 1000 cm^{-1} . The peaks at 1033 cm^{-1} were assigned to C–C skeleton vibration and C–O stretching vibration and were found in all biochars (Fig. S2(a, b, c)). The FTIR spectra provide the qualitative information of functional groups present on the surfaces of biochars. The results demonstrated the differences in surface functional groups between MSW^{sem} and SS^{sem} corresponding to different feedstock type and pyrolysis temperature. From Fig. S2(b), it is obvious that there were similar FTIR spectra between SS^{sem} , $\text{SS-KOH}^{\text{sem}}$, $\text{SS-H}_2\text{O}_2^{\text{sem}}$ with a small shift at 1635 cm^{-1} (SS^{sem}) to 1597 cm^{-1} ($\text{SS-KOH}^{\text{sem}}$).

Adsorption kinetics

The simulation of the sorption kinetics for Pb(II) by raw and modified biochars was performed using pseudo-first-order (Eq. 1) and pseudo-second-order (Eq. 2) kinetic models, which are illustrated as followed:

$$\log(Q_e - Q_t) = \log Q_e - \frac{k_1 t}{2.303} \quad (1)$$

$$\frac{t}{Q_t} = \frac{1}{k_2 Q_e^2} + \frac{t}{Q_e} \quad (2)$$

where Q_t and Q_e are Pb(II) adsorption capacity (mg g^{-1}) at time t (h) and equilibrium, k_1 (h^{-1}) and k_2 ($\text{g}(\text{mg h})^{-1}$) are the rate constants for pseudo-first-order and pseudo-second-order models, respectively (Liu & Zhang, 2009). The pseudo-first-order curves were plotted via $\log(Q_e - Q_t)$ versus time t in which the values of k_1 can be obtained from the slope corresponding to Eq. (1). The pseudo-second-order model was also applied to test the experimental data from the plot of t/Q_t against t , from which Q_e and k_2 values can be calculated from the slope and interception of this plot, respectively.

Adsorption isotherms

Langmuir and Freundlich models are presented in equation (3) and (4), respectively:

$$\frac{C_e}{Q_e} = \frac{1}{K_L Q_m} + \frac{C_e}{Q_m} \quad (3)$$

$$\ln Q_e = \ln K_F + \frac{1}{n} \ln C_e \quad (4)$$

where C_e is the equilibrium Pb solution concentration (mg L^{-1}), Q_e and Q_m are the Pb(II) adsorption capacity at equilibrium and at maximum capacity (mg g^{-1}), n is the Freundlich constant which indicates the favorability of adsorption, and K_L and K_F are the adsorption constants for the Langmuir and Freundlich isotherm models, respectively.

Evolution of pH during Pb adsorption isotherms

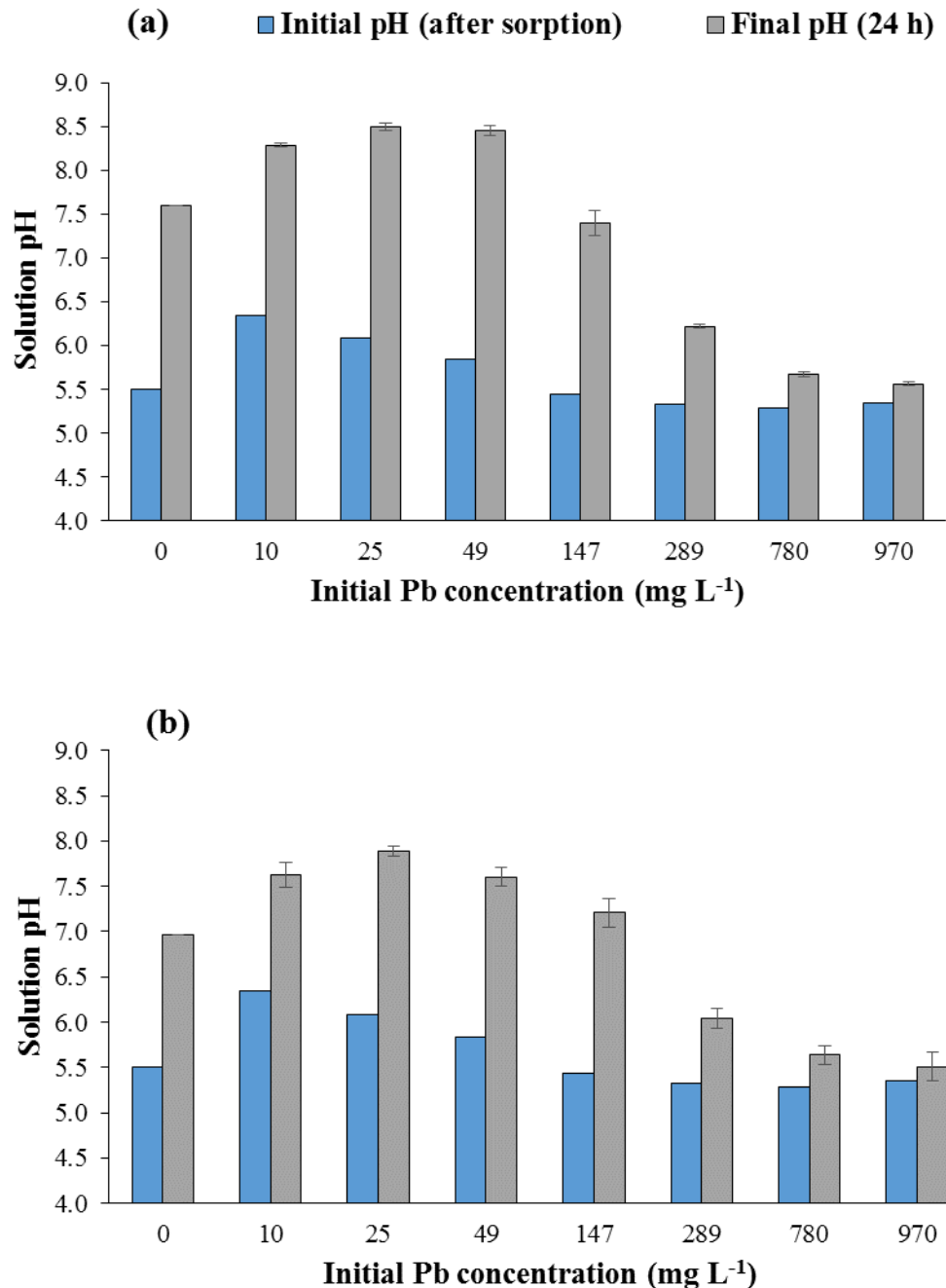


Fig. S3. The evolution of solution pH during Pb adsorption isotherms onto SS-KOH^{sem} (a) and MSW-KOH^{sem} (b).

Table S1.**Comparison of maximum adsorption capacities for lead by biochar produced from different waste materials.**

Biochar material	Pyrolysis temperature	Q_m (mg g ⁻¹)	Isotherm well-fitted model	Expiemental conditions: initial pH, biochar dosage	Reference
Peanut shell	350	52.8	Freundlich, Langmuir	pH 5, 4 g L ⁻¹	Wang et al. (2015)
Medicine material residues	350	46.1	Langmuir	pH 5, 4 g L ⁻¹	Wang et al. (2015)
Pine wood	300	3.9	Langmuir	pH 5, 4 g L ⁻¹	Liu & Zhang (2009)
Rice husk	300	1.8	Langmuir	pH 5, 4 g L ⁻¹	Liu & Zhang (2009)
Digested dairy waste	600	51.4	-	2 g L ⁻¹	Inyang et al. (2012)
Digested whole sugar beet	600	40.8	Langmuir	2 g L ⁻¹	Inyang et al. (2012)
Sewage sludge digestate	350	6.5	Langmuir	pH 5, 4 g L ⁻¹	This study
Organic fraction of municipal solid waste digestate	400	72.9	Langmuir	pH 5, 4 g L ⁻¹	This study

Table S2.

Chemical characteristics of the organic fraction of municipal solid waste digestate (RMSW), its derived biochar (MSW^{sem}), sewage sludge digestate (RSS) and its derived biochar (SS^{sem}).

Parameters	RMSW	MSW ^{sem}	RSS	SS ^{sem}
Biochar yield (% wt)	NA ^a	74 ± 1	NA	NA
Ash (% wt)	52 ± 1	68 ± 1	NA	NA
Moisture content (% wt)	81 ± 1	NA	NA	NA
As (mg kg ⁻¹) ^b	dl ^c	dl	79 ± 3 ^d	34 ± 12
Cd (mg kg ⁻¹)	dl	dl	dl	9 ± 1
Cr (mg kg ⁻¹)	94 ± 1	100 ± 2	42 ± 1	48 ± 1
Cu (mg kg ⁻¹)	261 ± 7	436 ± 5	390 ± 10	617 ± 7
Ni (mg kg ⁻¹)	43 ± 5	38 ± 3	25 ± 1	41 ± 1
Pb (mg kg ⁻¹)	101 ± 5	130 ± 12	80 ± 9	85 ± 3
Zn (mg kg ⁻¹)	693 ± 13	888 ± 12	756 ± 10	1017 ± 13

^a NA refers to not available.

^b Values reported on dry basis.

^c dl refers to below detection limit.

^d Values reported as means (n=3) followed by standard deviation.

Table S2 shows the metal(loid) contents of RMSW, MSW^{sem}, RSS and SS^{sem}. Metals such as Cr, Cu, Pb and Zn were retained in the biochars during pyrolysis, while As (metalloid) was volatilized at the temperature below 400 °C (Table S2), this was also affirmed by previous studies from Duan et al. (2017). As expected, Cu and Zn were the main components in both the solid digestates and biochars (Table S2), which was in correlation to the studies from Pituello et al. (2014). Additionally, no metals exceeded the limit values of metal(loid)s present in the sludge based on the French guidelines (Directive 86/278/EEC).

Table S3.

Parameters of pseudo-first-order and pseudo-second-order kinetics for lead sorption by SS^{sem}, SS-H₂O₂^{sem}, SS-KOH^{sem}, MSW^{sem}, MSW-H₂O₂^{sem} and MSW-KOH^{sem}.

Sample	Pseudo-first-order (PFO)				Pseudo-second-order (PSO)		
	$Q_{e,exp}$	Q_e	k_1	R^2	Q_e	k_2	R^2
SS ^{sem}	3.4	3.5	0.536	0.146	3.5	0.270	0.997
SS-H ₂ O ₂ ^{sem}	8.2	8.8	0.633	0.653	8.5	0.137	0.999
SS-KOH ^{sem}	13.7	13.9	1.780	NF ^a	14.0	1.057	0.999
MSW ^{sem}	23.7	24.2	4.287	0.990	23.8	0.735	0.999
MSW-H ₂ O ₂ ^{sem}	24.4	24.5	10.177	0.856	24.5	18.496	1.000
MSW-KOH ^{sem}	23.8	24.0	7.766	0.78	23.8	3.528	1.000

^aNF refers to no satisfactory fit by the model.

References

- Chen, X., Chen, G., Chen, L., Chen, Y., Lehmann, J., McBride, M.B., Hay, A.G., 2011. Adsorption of copper and zinc by biochars produced from pyrolysis of hardwood and corn straw in aqueous solution. *Bioresour. Technol.* 102, 8877–8884.
- Duan, L., Li, X., Jiang, Y., Lei, M., Dong, Z., Longhurst, P., 2017. Arsenic transformation behaviour during thermal decomposition of *P. vittata*, an arsenic hyperaccumulator. *J. Anal. Appl. Pyrolysis* 124, 584–591.
- Inyang, M., Gao, B., Yao, Y., Xue, Y., Zimmerman, A.R., Pullammanappallil, P., Cao, X., 2012. Removal of heavy metals from aqueous solution by biochars derived from anaerobically digested biomass. *Bioresour. Technol.* 110, 50–56.
- Jouraiphy, A., Amir, S., El Gharous, M., Revel, J.C., Hafidi, M., 2005. Chemical and spectroscopic analysis of organic matter transformation during composting of sewage sludge and green plant waste. *Int. Biodeterior. Biodegrad.* 56, 101–108.
- Liu, Z., Zhang, F.S., 2009. Removal of lead from water using biochars prepared from hydrothermal liquefaction of biomass. *J. Hazard. Mater.* 167, 933–939.
- Pituello, C., Francioso, O., Simonetti, G., Pisi, A., Torreggiani, A., Berti, A., Morari, F., 2014. Characterization of chemical–physical, structural and morphological properties of biochars from biowastes produced at different temperatures. *J. Soils Sediments* 15, 792–804.
- Wang, Z., Liu, G., Zheng, H., Li, F., Ngo, H.H., Guo, W., Liu, C., Chen, L., Xing, B., 2015. Investigating the mechanisms of biochar's removal of lead from solution. *Bioresour. Technol.* 177, 308–317.